



Contents lists available at ScienceDirect

Chemical Data Collections

journal homepage: www.elsevier.com/locate/cdc

Synthesis, spectral characterization, crystal structure and theoretical investigation of (*E*)-3-(4-bromothiophen-2-yl)-1-(5-bromothiophen-2-yl)prop-2-en-1-one

B. Pramodh^{a,†}, P. Naresh^{b,†}, S. Naveen^{c,*}, N.K. Lokanath^{b,*}, S. Ganguly^d, J. Panda^e, S. Murugesan^f, A.V. Raghu^g, Ismail Warad^h

^a Department of Studies in Physics, Manasagangotri, University of Mysore, Mysuru 570006, India

^b GITAM Institute of Pharmacy, GITAM (Deemed-to-be University), Rushikonda, Visakhapatnam-530045, India

^c Department of Physics, Faculty of Engineering & Technology, Jain (Deemed-to-be University), Bangalore 562 112, India

^d Department of Pharmaceutical Sciences and Technology, Birla Institute of Technology, Mesra, Ranchi- 835215, Jharkhand, India

^e Raghu College of Pharmacy, Dakamarri, Bheemunipatnam, Visakhapatnam-531162, India

^f Medicinal Chemistry Research Laboratory, Department of Pharmacy, Birla Institute of Technology & Science Pilani, Pilani Campus, Pilani-333031, Rajasthan, India

^g Department of Chemistry, Faculty of Engineering & Technology, Jain (Deemed-to-be University), Bangalore 562 112, India

^h Department of Chemistry and Earth Sciences, PO Box 2713, Qatar University, Doha, Qatar

ARTICLE INFO

Article history:

Received 29 June 2020

Revised 14 October 2020

Accepted 28 October 2020

Available online 5 November 2020

Keyword:

Chalcone

X-ray diffraction

Hirshfeld surface analysis and DFT studies

ABSTRACT

Chalcone derivatives have been attracting significant attention due to their various pharmacological activities. Changes in their structures have displayed high degree of diversity that has proven to result in a broad spectrum of biological activities. The present study highlights the synthesis of chalcone containing the bromo-thiophene moiety and spectroscopically characterized by FT-IR, NMR and the crystal structure was confirmed by X-ray diffraction method. The compound, C₁₁H₆Br₂OS₂ crystallizes in monoclinic system with space group *P*2₁/*n*. The crystal structure revealed the supramolecular ring motif *R*₂²(6) and *R*₂²(10). The Hirshfeld surface analysis quantifies the intermolecular interactions involved in the crystalline environment. The molecular geometry was optimized using density functional theory at B3LYP/6-311G+(d, p) level basis set to substantiate the experimental results. Further, the frontier molecular orbital analysis revealed the electro-chemical parameters. The molecular electrostatic potential map and atomic charge analysis identifies the positive, negative and neutral reactive sites in the molecular system.

© 2020 Elsevier B.V. All rights reserved.

* Corresponding authors.

E-mail addresses: s.naveen@jainuniversity.ac.in (S. Naveen), lokanath@physics.uni-mysore.ac.in (N.K. Lokanath).

† These authors contributed equally.

Specifications Table

Subject area	Organic Chemistry and X-ray Crystallography
Compound	3-(4-bromothiophen-2-yl)-1-(5-bromothiophen-2-yl)prop-2-en-1-one
Data category	Spectral, synthesis, crystallographic data
Data acquisition format	FT-IR, NMR, X-ray diffraction studies
Data type	Analyzed and simulated
Procedure	The compound was synthesized by adding a mixture of ketone (2-acetyl-5-bromo-thiophene) (1 g, 4.85 mmol), 4-bromo-thiophene-2-carboxaldehyde (0.92 g, 4.85 mmol), in ethanol (25 mL) and was treated with lithium hydroxide monohydrate (LiOH•H ₂ O) (20.37 mg, 0.485 mmol). The reaction mixture was then poured over crushed ice and acidified with dilute HCl and the solid which precipitated was filtered and washed with water, dried to obtain pure green crystals.
Data accessibility	CCDC No: 2012717 URL: https://www.ccdc.cam.ac.uk/conts/retrieving.html

1. Rationale

Chalcone is a simple scaffold of many naturally occurring compounds, and acts as the central core of various important biological compounds [1]. In chalcone derivatives the aromatic substituents are introduced in to the terminal position of the C=C-C=O system. Chalcones belongs to family of bicyclic flavonoids, defined by the presence of two aromatic rings linked by a three carbon unit, forming an α , β -unsaturated carbonyl group [2,3]. The α , β -unsaturated carbonyl system of chalcones possesses two electrophilic reactive centers allowing them to participate in addition reactions via attack to the carbonyl group (1,2-addition) or involving the β -carbon (1,4-conjugate addition), leading to the synthesis of promising bioactive heterocyclic compounds [4]. The chemistry of chalcones has developed intensive scientific studies throughout the world. Chalcones exist as either *E* or *Z* isomers, the *E*-isomer being in most cases the thermodynamically most stable form and consequently, the majority of the chalcones is isolated as the *E*-isomer [5].

Chalcone derivatives have attracted significant attention in the past few decades due to their availability of many useful properties including anti-bacterial [6], anti-viral [7], anti-fungal [8], anti-cancer [9], anti-inflammatory [10], anti-tubercular [11], anti-hyperglycemic [12], anti-malarial agents [13], among others. Also, the Chalcone derivatives readily form the supramolecular synthons, so that variety of novel heterocycles with good pharmaceutical profile can be obtained [14]. Chalcones can be used as intermediates in the synthesis of many pharmaceutically useful molecules [15]. Given such varied pharmacological activities and synthetic utilities, chalcones derivatives have always attracted chemists to develop new molecules and study their biological activities.

In view of variety of applications associated with the chalcone derivatives and as a part of our research on novel chalcones [16–19], herein we report the synthesis, spectral characterization, molecular and crystal structure, Hirshfeld surface analysis and theoretical (DFT) studies of (E)-3-(4-bromothiophen-2-yl)-1-(5-bromothiophen-2-yl)prop-2-en-1-one.

2. Procedure

2.1. Materials and methods

All the aldehydes and the ketone (2-acetyl-5-bromo-thiophene) were purchased from Sigma Aldrich India and Merck India. Lithium hydroxide monohydrate (LiOH•H₂O) was procured from Sisco Research Laboratories (India). All the reagents were used without purification and solvents used were commercial as well as analytical grade. The IR spectra of the title compound was recorded on a Bruker FTIR spectrophotometer. ¹H NMR spectra were recorded on a Bruker Avance DRX400 (400 MHz, FTNMR) in CDCl₃ solvent. The progress of the reaction was monitored by TLC in a solvent-vapor-saturated chamber on glass plates coated with Silica Gel GF₂₅₄, followed by visualization under UV light (254 nm). The solvent system used for thin layer and column chromatography was *n*-hexane: ethyl acetate (8:2). Sonication was performed using an ultrasonic cleaner (with a frequency of 50 Hz and a nominal power 170 W). The X-ray diffraction data were collected using Rigaku XtaLAB diffractometer.

2.2. Synthesis of the (E)-3-(4-bromothiophen-2-yl)-1-(5-bromothiophen-2-yl)prop-2-en-1-one

A mixture of ketone (2-acetyl-5-bromo-thiophene) (1 g, 4.85 mmol), 4-bromo-thiophene-2-carboxaldehyde (0.92 g, 4.85 mmol), in ethanol (25 mL) was treated with lithium hydroxide monohydrate (LiOH•H₂O) (20.37 mg, 0.485 mmol). The mixture was irradiated in the water bath of an ultrasonic cleaner at the room temperature for a period of 30 min or until a precipitate was formed. The reaction mixture was then poured over crushed ice and acidified with dilute HCl and the solid which precipitated was filtered and washed with water, dried and was purified on column chromatography (silica gel with 10% ethyl acetate in hexane) to get pure green crystals (Scheme 1 Yield: 1.8 g (93%), mp: 126 °C. The reaction pathway is shown in Fig. 1.

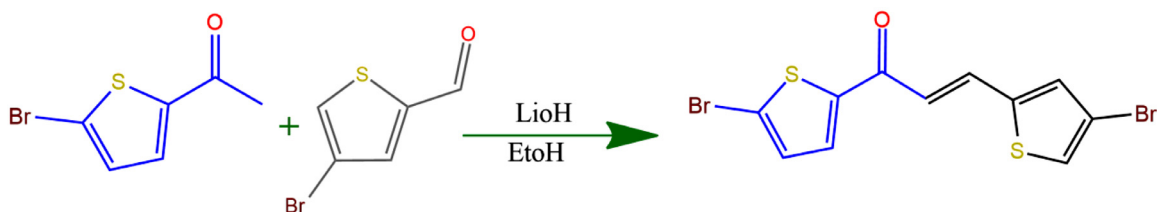


Fig. 1. Reaction path way of the synthesized title compound.

Table 1
Crystal data and structure refinement detail.

Parameter	Values
CCDC Number	2012717
Empirical formula	C ₁₁ H ₆ Br ₂ OS ₂
Formula weight	378.10
Temperature (K)	293(2)
Radiation	MoK α
Wavelength (\AA)	0.71073
Crystal system, space group	Monoclinic, $P2_1/n$
a (\AA)	4.051(12)
b (\AA)	15.701(4)
c (\AA)	19.817(5)
α ($^\circ$)	90.00
β ($^\circ$)	95.572(16)
γ ($^\circ$)	90.00
Volume (\AA^3)	1257.6(6)
Z	4
Density(calculated) Mg m ⁻³	2.002
Absorption coefficient mm ⁻¹	6.768
F_{000}	728
Crystal size (mm)	0.27 \times 0.25 \times 0.23
θ range for data collection	3.32 $^\circ$ to 23.81 $^\circ$
Index ranges	-4 $\leq h \leq$ 4 -17 $\leq k \leq$ 17 -13 $\leq l \leq$ 22
Reflections collected	3848
Independent reflections	1885 [$R_{\text{int}} = 0.1874$]
Data collection diffractometer	Rigaku
Absorption correction	Multi-scan
Refinement method	Full matrix least-squares on F^2
Data / restraints / parameters	1885/ 0 / 145
Goodness-of-fit	0.953
$R1, wR2$ [$I > 2\sigma(I)$]	0.0887, 0.2124
$R1, wR2$ [all data]	0.1126, 0.2322
Residual (e \AA^{-3})	1.065 and -1.843

2.3. X-Ray diffraction studies

A single crystal suitable for X-ray crystallographic study was selected using a polarizing microscope and mounted on goniometer. The X-ray diffraction data were collected at room temperature using Rigaku XtaLAB Mini CCD diffractometer equipped with X-ray generator operating at 45 kV, 12 mA, CCD area detector and fine-focus sealed tube with a graphite monochromator using MoK α ($\lambda = 0.71073 \text{ \AA}$) radiation. Data were collected with χ fixed at 54 $^\circ$, for different settings of φ (0 $^\circ$ and 360 $^\circ$), keeping the scan width of 0.5 $^\circ$ with exposure time of 4 s and the sample to detector distance was fixed to 50 mm. Data collection and reduction were performed using Crystal Clear program [20,21].

The structure was solved by direct methods with SHELXS [22] and refined by a full-matrix least-squares technique on F^2 using SHELXL-2014 [23] with anisotropic thermal parameters for the non-H atoms. All Hydrogen atoms were located using difference Fourier techniques and refined with isotropic temperature factors. The geometric calculations were carried out using the program PLATON [24] and the packing diagram was generated using MERCURY program [25]. The crystal data and structure refinement summaries are given in Table 1.

2.4. Quantum computational studies

The quantum chemical computational studies help to investigate the electrochemical properties of the molecules. The crystallographic information file was used as the input for the optimization of the structural coordinates. The molecular

Table 2

Theselected bond lengths (Å), bond angles (°) and torsion angles (°) of the title compound obtained from experimental (XRD) and theoretical (DFT) methods.

Atoms	Bond length (Å)		Atoms	Bond Angles (°)		Atoms	Torsional Angles (°)	
	XRD	DFT		XRD	DFT		XRD	DFT
Br16–C14	1.89(1)	1.8872	C11–S15–C14	90.2(5)	90.56	C14–S15–C11–C9	180.0(9)	178.82
Br1–C2	1.90(1)	1.9024	C5–S4–C3	92.2(6)	91.89	C14–S15–C11–C12	1.0(9)	1.64
S15–C11	1.75(1)	1.7505	S15–C11–C9	116.9(8)	117.70	C11–S15–C14–C13	-0.4(9)	-1.24
S15–C14	1.70(1)	1.7315	S4–C5–C6	110.8(9)	110.40	C3–S4–C5–C6	2.3(9)	3.89
S4–C5	1.72(1)	1.7535	C6–C5–C7	127(1)	125.72	C12–C11–C9–C8	6(2)	4.8
S4–C3	1.73(1)	1.7307	C9–C8–C7	122(1)	119.90	S15–C11–C12–C13	-1(1)	-1.68
O10–C9	1.21(1)	1.2268	O10–C9–C11	120(1)	120.02	C9–C11–C12–C13	180(1)	178.86
C11–C9	1.45(1)	1.4755	O10–C9–C8	121(1)	122.18	S4–C5–C6–C2	-2(1)	-3.05
C11–C12	1.35(2)	1.3794	C5–C6–C2	112(1)	112.62	S4–C5–C7–C8	5(2)	2.06
C5–C6	1.38(1)	1.379	S4–C3–C2	109.7(9)	110.94	C6–C5–C7–C8	178(1)	178.76
C5–C7	1.44(2)	1.4428	Br16–C14–C13	126.9(9)	125.93	C7–C8–C9–C11	174(1)	175.63
C8–C9	1.47(1)	1.482	S15–C14–C13	114.3(9)	113.29	C9–C8–C7–C5	179(1)	179.86
C8–C7	1.29(2)	1.3489	Br1–C2–C6	122.5(8)	122.88	C5–C6–C2–Br1	-177.7(8)	-178.74
C6–C2	1.39(2)	1.4189	C6–C2–C3	115(1)	113.96	C5–C6–C2–C3	1(2)	0.23
C3–C2	1.35(2)	1.3653	C11–C12–C13	115(1)	113.70	S4–C3–C2–Br1	179.4(6)	178.29
C14–C13	1.33(2)	1.3718	C14–C13–C12	111(1)	111.40	S15–C14–C13–C12	-0(1)	0.52
C12–C13	1.39(2)	1.4191	C5–C7–C8	129(1)	127.31	C11–C12–C13–C14	1(2)	0.77
Correlation coefficient = 0.9972			Correlation coefficient = 0.9958			Correlation coefficient = 0.9998		

geometry optimization and the quantum chemical calculations of the title compound were carried out using Gaussian-16 software [26]. The frontier molecular orbital energies (E_{HOMO} and E_{LUMO}), electronic properties and Mulliken's atomic charges were calculated using density functional theory by B3LYP hybrid functional with 6-311+G(d, p) basis set. The molecular electrostatic potential (MEP) map and the frontier molecular orbitals were visualized using Gauss View 6.0.16 [27] software. The Hirshfeld surface analysis was carried out using Crystal Explorer 17 [28] program to explore the intermolecular interaction involved in the crystal environment.

3. Data, value and validation

3.1. Spectral characterization FTIR and NMR analysis

The FTIR spectra of the synthesized titled compound were recorded on a Bruker FTIR spectrophotometer. The characteristic vibrational frequency observed in the FT-IR spectrum supports the structure of the title compound as shown in Fig. S1. The low intensity absorption bands around the region of 2855 cm^{-1} to 3085 cm^{-1} are attributed to aromatic C–H stretching, however the strong intensity bands at the region around 1408 cm^{-1} to 1588 cm^{-1} are attributed to aromatic C=C stretching vibrations of thiophene rings. The characteristic ketone peak of α , β -unsaturated carbonyl (chalcone) was observed at 1639 cm^{-1} . A strong intense peak at 585 cm^{-1} indicates the presence of C–Br stretch. The bending mode vibration of C–S was identified at 789 cm^{-1} and 869 cm^{-1} that indicates the presence of thiophene.

^1H NMR spectrum of the titled compound (E)-3-(4-bromothiophen-2-yl)-1-(5-bromothiophen-2-yl)prop-2-en-1-one was recorded on Bruker Avance DRX400 (400 MHz, FTNMR) in CDCl_3 shows the proposed structural formula shown in Fig. 1. As the proposed structure contains two thiophene rings thus, the protons associated with the carbons falls under aromatic region. Several peaks in the aromatic region from δ 7.15 to δ 7.85 ppm were assigned to aromatic thiophene protons as shown in Fig. S2. The ^1H NMR of the novel chalcone has shown a multiplet, at a range of δ 7.56–7.57 ppm (for H_β) and another at a range of δ 7.08–7.12 ppm (for H_α) for vinylic protons nearer the carbonyl group ($-\text{CH}_\beta=\text{CH}_\alpha-\text{C}=\text{O}$). Interestingly for the title compound we found the coupling constants value (J) of $J_{\text{H}_\alpha-\text{H}_\beta} = 15.0\text{ Hz}$, that confirms the *trans* configuration of the vinylic system.

3.2. Single crystal X-ray diffraction analysis

The compound crystallizes in the monoclinic system in the $P2_1/n$ space group with the cell parameters $a = 4.051(12)\text{ \AA}$, $b = 15.701(4)\text{ \AA}$, $c = 19.817(5)\text{ \AA}$ and $\alpha = \gamma = 90.00^\circ$, $\beta = 95.572(16)^\circ$ and $Z = 4$. The ORTEP of the molecule with thermal ellipsoids drawn at 50% probability and DFT optimized geometrical structure of the title compound is as shown in Fig. 2. The theoretical parameters obtained from the DFT calculations with B3LYP/6-311G+(d,p) provide the complete information of the molecular geometry. The theoretically calculated structural parameters are compared with the experimental values with good correlation coefficient (bond length **0.9972**, bond angles **0.9958** and torsion angles **0.9998**) and are listed in Table 2.

The structure has one molecule in the asymmetric unit and four molecules per unit cell. The non-planarity is confirmed by a dihedral angle of (9.05°) between the two bromo-thiophene rings. The details of crystal structure and data refinement

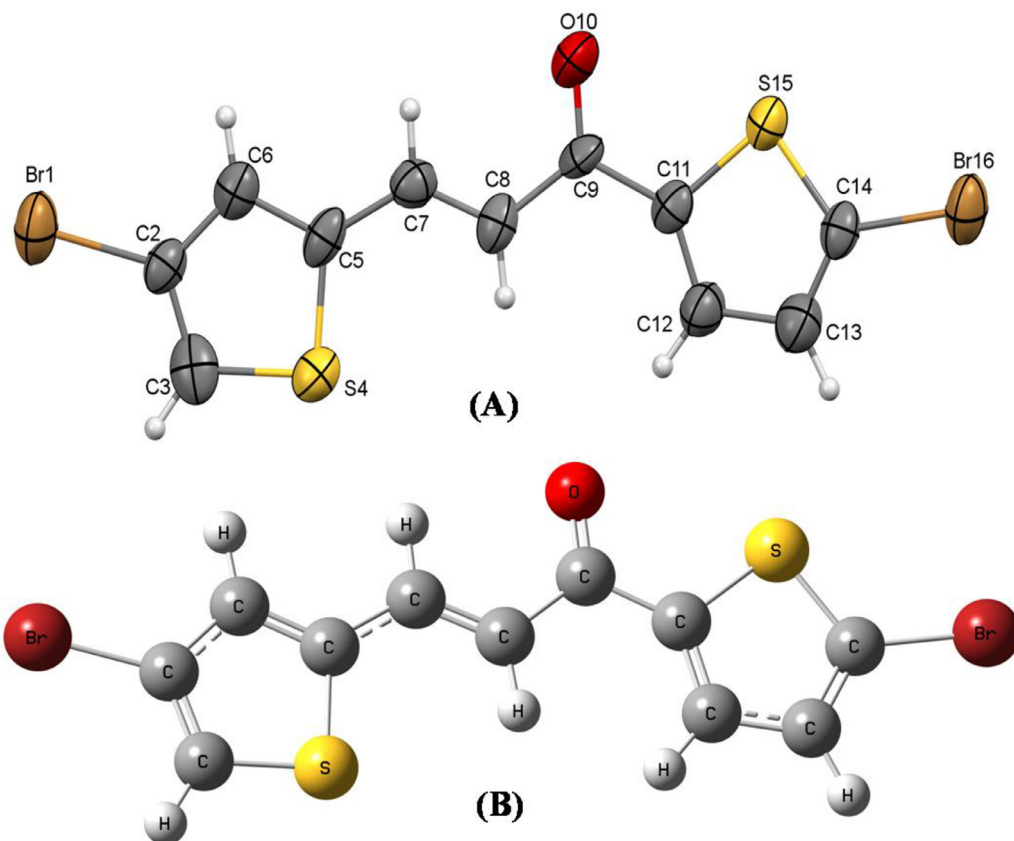


Fig. 2. (A) ORTEP of the molecule with thermal ellipsoids drawn at 50% probability and (B) DFT optimized molecular structure of the title compound.

Table 3
The hydrogen bond geometry of the title compound.

No.	Type	D-H...A	H...A (Å)	D...A (Å)	D-H...A (°)
1	Inter ⁱ	C6-H6...O10	2.454	3.303(14)	140
2	Inter ⁱ	C7-H7...O10	2.51	3.329(14)	102
3	Intra	C8-H8...S4	2.86	3.210(12)	104

Symmetry codes: (i) $1-x, 1-y, 1-z$

parameters are given in **Table 1**. The compound exhibits *E*-conformation with respect to ketone bond. The molecules are connected in a zig-zag manner along the *c*-axis as shown in **Fig. S3**. The compound exhibits C9–O10...Cg(2) interaction with a distance of 3.867(9) Å (where Cg(2) is the centroid of the ring S15/C11/C12/C13C14). The two intermolecular interactions C–H...O and C–H...S stabilize the crystal structure and are listed in **Table 3**.

The crystal structure exhibits C–H...O and C–H...S type of intramolecular hydrogen bond interactions which greatly contributes to the stability of the crystal structure. These interactions lead to the formation of supramolecular synthons of the type $R_2^1(6)$ and $R_2^2(10)$ as depicted in **Fig. 3**.

4. Theoretical calculations

4.1. Hirshfeld surface analysis

The Hirshfeld surface analysis plays an important role in understanding the intermolecular interactions in the crystal structure. The short contact was analyzed by Hirshfeld surface generated using Crystal Explorer [28]. The bright circular red spots on d_{norm} Hirshfeld surface indicates the presence of strong C–H...O interaction, which corresponds to the C6–H6...O10 and C7–H7...O10 hydrogen bonds as shown in **Fig. 4**, whereas the blue area represents completely free from the close contacts. The Hirshfeld surface analysis of molecular structure shows Br...H interaction contributes 21.40%, C...H interaction contributes 14%, Br...S interaction contributes 13.70%, H...H contact contributes 11.60%, to the total in-

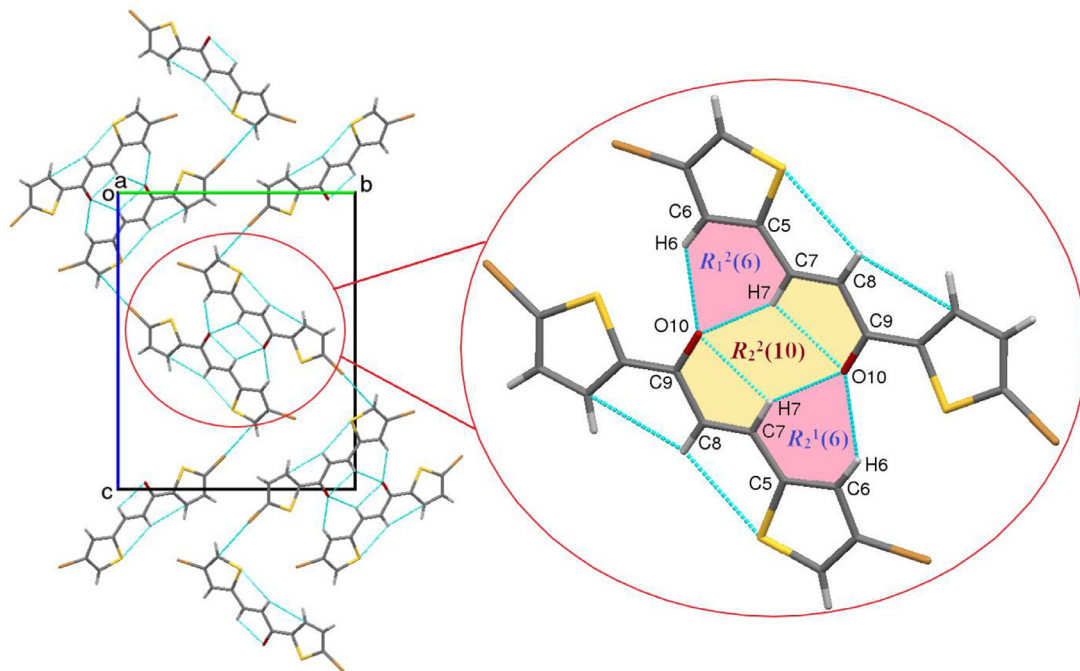


Fig. 3. The packing of the molecule viewed along *a*-axis and supramolecular ring motif.

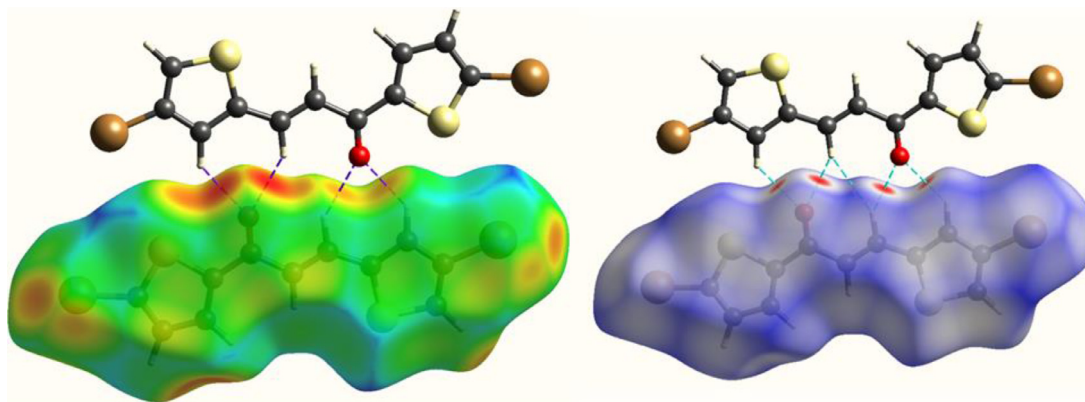


Fig. 4. Hirshfeld surface mapped with shape index and d_{norm} of the title compound.

teractions and plays an important role in stabilizing the crystal structure. Further, the 2D-finger plots and the percentage contributions of other weak interactions are shown in Fig. 5.

4.2. Geometry optimization and frontier molecular orbitals (FMOs)

The optimized geometrical structure is shown in Fig. 2(B). The bond length, bond angles and torsional angles are in good correlation with the experimental values as tabulated in Table 2. The frontier molecular orbital theory allows a chemist to make predictions about a reaction by knowing the distribution of orbital energy levels. The molecular coordinates of structure was optimized by the density functional theory (DFT) using B3LYP hybrid functional with 6-311+G(d,p) basis set. The intermolecular charge transfer process in molecular system from a donor to acceptor moiety is characterized by the excitation of an electron from occupied orbital (HOMO) to unoccupied orbital (LUMO) and explained by quantum chemical method approach [29]. A high HOMO energy level represents a compound that is a good nucleophile and a low LUMO level represents a compound that is a good electrophile [30]. The frontier molecular orbital energies are as shown in the Fig. 6.

The calculated energies of the HOMO and LUMO can be used to obtain the electrochemical parameter such as global electrophilicity index (ω), global hardness (h), chemical potential (μ) and global softness (S) were referred as global reactivity parameters [31–35]. Also, the magnitudes of electrophilicity index can be used as possible descriptor for bioactivity of the

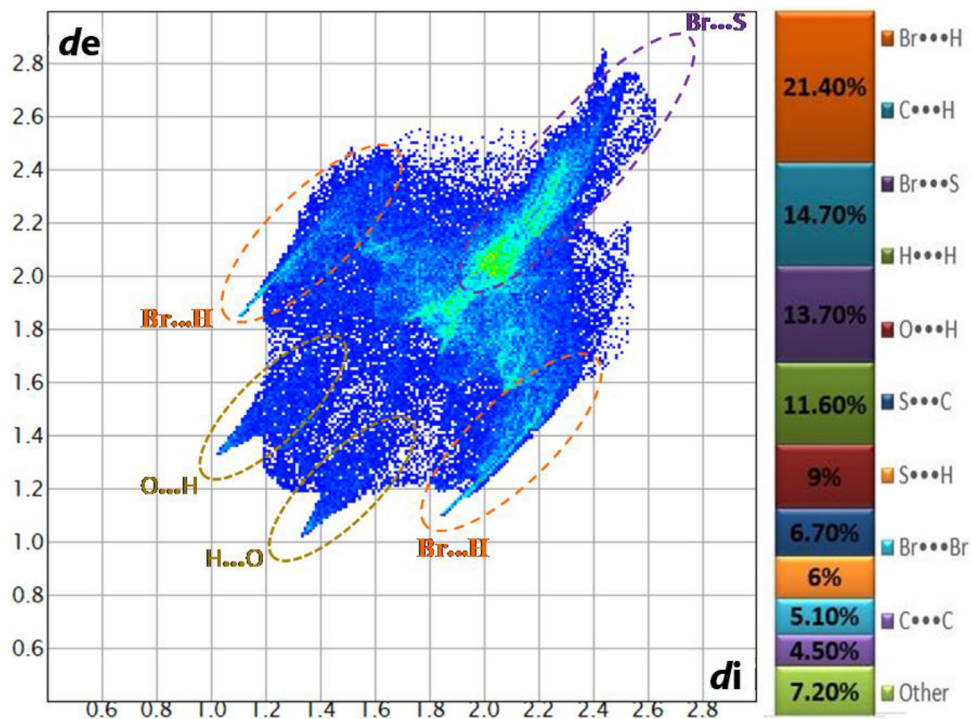


Fig. 5. 2D-finger print plots and relative contributions of various interactions of the title molecule. Here d_i is the closest internal distance from a given point on the Hirshfeld surface and d_e is the closest external contacts.

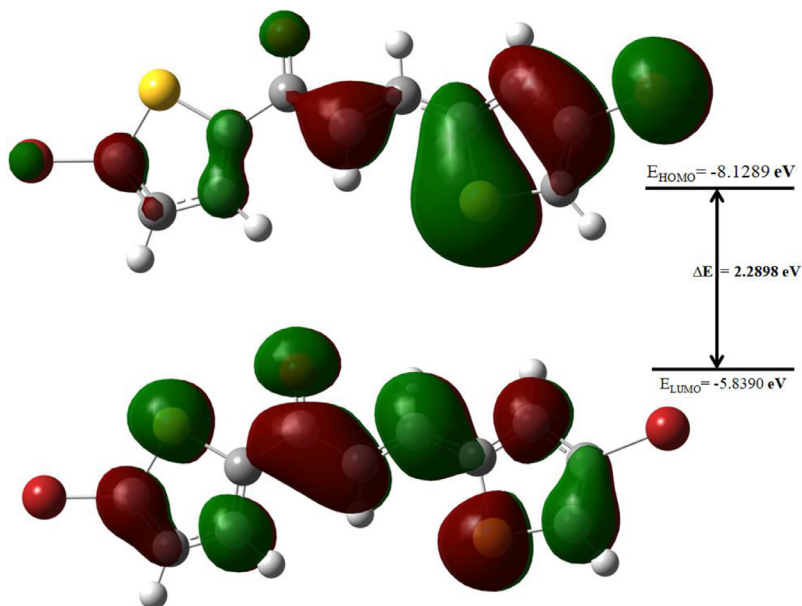


Fig. 6. Frontier molecular orbital energies

chemical systems [36]. The frontier molecular orbital (HOMO-LUMO) energies can be obtained as $I = -E_{\text{HOMO}}$ and $A = -E_{\text{LUMO}}$ respectively. The hardness and softness have been connected with the stability and chemical reactivity of the system [37]. The quantum chemical descriptors are listed in Table 4.

Table 4
Quantum chemical descriptors of the title compound.

Parameter	Value
E_{HOMO}	-8.1289(eV)
E_{LUMO} (eV)	-5.8390(eV)
Energy gap (E_g)	2.2898(eV)
Ionization energy (I)	8.1289(eV)
Electron affinity (A)	5.8390(eV)
Electronegativity (χ)	6.9839(eV)
Chemical potential (μ)	-6.9839(eV)
Global hardness (η)	1.1449(eV)
Global softness (S)	0.8734(eV ⁻¹)
Electrophilicity index (ω)	21.3008(eV)

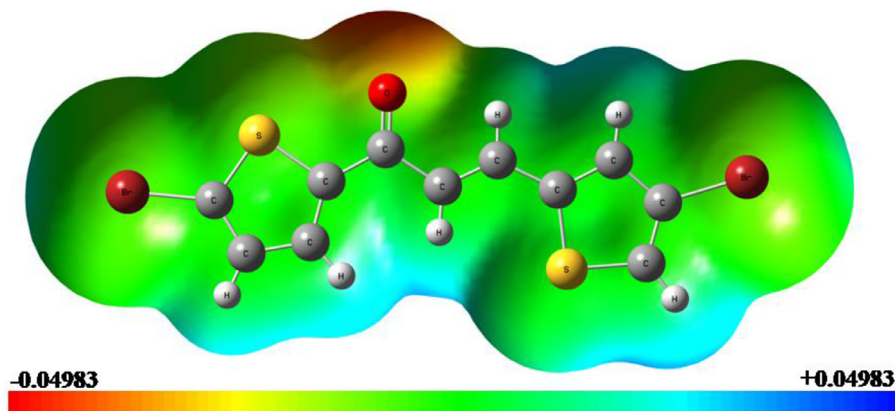


Fig. 7. Molecular electrostatic potential map of the title compound.

4.3. Molecular electrostatic potential analysis

The molecular electrostatic potential (MEP) maps are very useful three dimensional diagrams which are used to visualize the charge distributions and physicochemical features of the molecules. Also, MEP picture has been used to predict electrophilic, nucleophilic and neutral electrostatic potential regions, in terms of color grading and useful in suites of the molecular structure and physicochemical property relationship and in studies of biological recognition and hydrogen bonding interactions [38,39]. The MEP of the title compound was calculated theoretically at the B3LYP/6-311+G (d,p) level basis set and obtained plots are shown in Fig. 7.

In the title compound, the negative potential region with red color spread over oxygen atoms indicating the electrophilic nature, hence the reactive sites are present near the C=O group. The negative potential values of the compound around the carbonyl oxygen atom indicates (-0.04983 a.u.) the strongest repulsive nature (electrophilic reactive site). The most positive region is localized on the hydrogen atoms and shows the strongest attraction (nucleophilic reactive sites) in the molecular system.

4.4. Mulliken atomic charge analysis

Mulliken atomic charge analysis helps in understanding the chemical and ionization potential. Atomic charge influences the dipole moment, polarizability electronic structure and difference molecular properties of the system [40]. Mulliken atomic charges with hydrogens summed into heavy atoms were calculated using B3LYP/6-311G+(d,p) basis set method and are plotted in Fig. 8. The atomic charges calculations showed that the carbonyl group connects between the two thiophene ring have clearly affected electronic charge. As expected, the presence of ketone moiety increased the electronegativity of the C9 atom.

5. Conclusion

The title compound (*E*)-3-(4-bromothiophen-2-yl)-1-(5-bromothiophen-2-yl)prop-2-en-1-one has been synthesized and characterized spectroscopically by FT-IR, NMR techniques. The crystals of the compound were grown by slow evaporation method and then the molecular structure was confirmed by single crystal X-ray diffraction studies. The title compound crystallized in the monoclinic system with space group $P2_1/n$. The crystal structure exhibits both inter and intramolecular

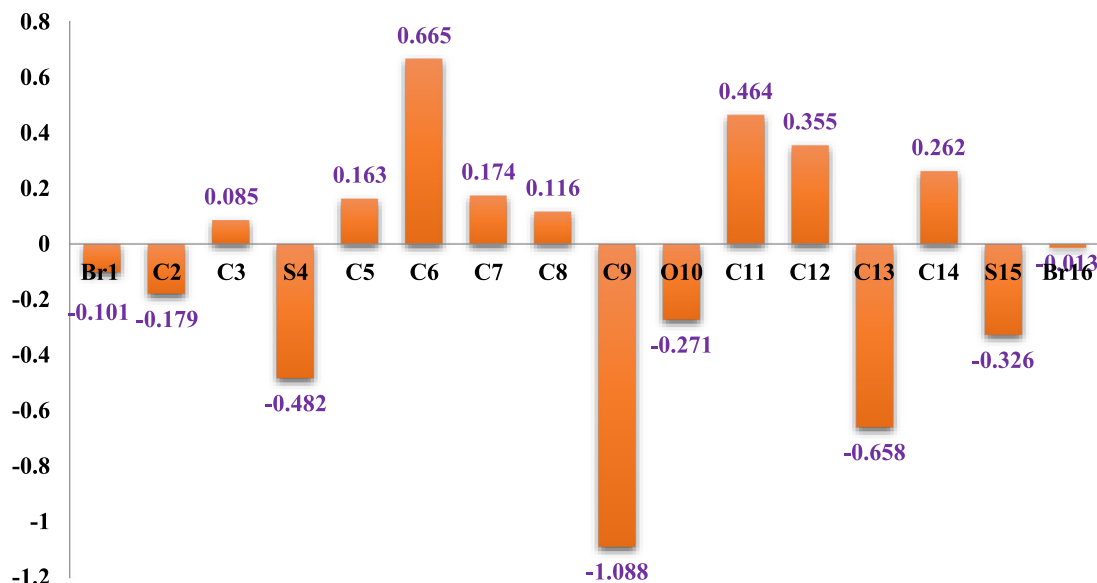


Fig. 8. The Mulliken atomic charge distributions of the title compound.

hydrogen bond interactions of the type C–H•••O, C–H•••S apart from the C–O••• π interaction. These interaction leads to the formation of supramolecular $R_2^2(6)$ and $R_2^2(10)$ ring motif. The Hirshfeld surface analysis with 3D d_{norm} and 2D-finger print plot revealed the various intermolecular interactions Br•••H (21.4%), Br•••S (13.70%) and C•••H (14.70%) involved in stabilizing the crystal structure. Further, structural parameters obtained by DFT calculations were well agreed with the experimental parameters. The HOMO-LUMO energy gap of the compound is found to be 2.2829 eV. Finally, the molecular electrostatic potential map and the atomic charge analysis explored the reactive nucleophilic, electrophilic sites on the molecular surface. The most negative potential region with red color spread over the oxygen atoms and the positive potential with blue color region are concentrated around the hydrogens of carbon atoms.

Declaration of Competing Interest

None.

Acknowledgements

The authors are grateful to and dedicate this article to commemorate the 25th year of the National Single Crystal Diffractometer Facility, Department of Studies in Physics, University of Mysore, Manasagangotri, Mysuru for providing X-ray intensity data. The authors acknowledge the financial support of UGC-IOE and DST -PURSE projects.

Supplementary materials

Supplementary material associated with this article can be found, in the online version, at [doi:10.1016/j.cdc.2020.100587](https://doi.org/10.1016/j.cdc.2020.100587).

References

- [1] A.Rammohan, J.S. Reddy, G. Sravya, C.N. Rao, Zyryanov, Chalcone synthesis, properties and medicinal applications: a review, *Environ. Chem. Lett.* 18 (2020) 1–26, doi:10.1007/s10311-019-00959-w.
- [2] Y. Nakamura, S. Watanabe, N. Miyake, H. Kohno, T. Osawa, Dihydrochalcones: evaluation as novel radical scavenging antioxidants, *J. Agric. Food. Chem.* 51 (2003) 3309–3312, doi:10.1021/jf0341060.
- [3] Y.P. Qian, Y.J. Shang, Q.F. Teng, Hydroxychalcones as potent antioxidants: Structure–activity relationship analysis and mechanism considerations, *Food. Chem.* 126 (2011) 241–248, doi:10.1016/j.foodchem.2010.11.011.
- [4] M.T. Albuquerque, C. Santos, A.S. Cavaleiro, A. Silva, Chalcones as versatile synthons for the synthesis of 5- and 6-membered nitrogen heterocycles, *Curr. Org. Chem.* 18 (2014) 2750–2775, doi:10.2174/1385272819666141013224253.
- [5] M. Larsen, H. Kromann, A. Kharazmi, S.F. Nielsen, Conformationally restricted anti-plasmodial chalcones *Bioorg. Med. Chem. Lett.* 15 (2005) 4858–4861, doi:10.1016/j.bmcl.2005.07.012.
- [6] X.F. Liu, C.J. Zheng, L.P. Sun, X.K. Liu, H.R. Piao, Synthesis of new chalcone derivatives bearing 2,4-thiazolidinedione and benzoic acid moieties as potential anti-bacterial agents, *Eur. J. Med. Chem.* 46 (2011) 3469–3473, doi:10.1016/j.ejmech.2011.05.012.
- [7] H. Terashima, K. Hama, R. Yamamoto, M. Tsuboshima, R. Kikkawa, I. Hatanaka, Y. Shigeta, Effects of a new aldose reductase inhibitor on various tissues *in vitro*, *J. Pharmacol. Exp. Therapeut.* 229 (1984) 226–230.
- [8] Z.N. Siddiqui, S. Praveen, T.N. Musthafa, A. Ahmad, A.U. Khan, Thermal solvent-free synthesis of chromonyl chalcones, pyrazolines and their *in vitro* antibacterial, antifungal activities, *Enzyme Inhib. Med. Chem.* 27 (2012) 84–91, doi:10.3109/14756366.2011.577035.

- [9] S.A. Rostom, M.H. Badr, H.A. Abd El Razik, H.M. Ashour, A.E. Abdel Wahab, Synthesis of some pyrazolines and pyrimidines derived from polymethoxy chalcones as anticancer and antimicrobial agents. *Arch. Pharm.* 344(2011) 572–587. <https://doi.org/10.1002/ardp.201100077>
- [10] L.D. Chiaradia, P.G. Martins, R.V. Guido, M.N. Cordeiro, G. Ecco, A.D. Andricopulo, R.A. Yunes, J. Vernal, R.J. Nunes, H. Terenzi, Synthesis, biological evaluation, and molecular modeling of chalcone derivatives as potent inhibitors of *Mycobacterium tuberculosis* protein tyrosine phosphatases (PtpA and PtpB). *J. Med. Chem.* 55 (2012) 390–402, doi:10.1021/jm2012062.
- [11] Y.M. Lin, Y. Zhou, M.T. Flavin, L.M. Zhou, W. Nie, F.C. Chen, Chalcones and flavonoids as anti-tuberculosis agents, *Bioorg. Med. Chem.* 10 (2002) 2795–2802, doi:10.1016/S0968-0896(02)00094-9.
- [12] P. Shukla, A.B. Singh, A.K. Srivastava, R. Pratap, Chalcone based aryloxypropanolamines as potential antihyperglycemic agents, *Bioorg. Med. Chem. Lett* 17 (2007) 799–802, doi:10.1016/j.bmcl.2006.10.068.
- [13] C.E. Gutteridge, J.V. Vo, C.B. Tillett, J.A. Vigilante, J.R. Dettmer, S.L. Patterson, L. Gerena, Antileishmanial and antimalarial chalcones: synthesis, efficacy and cytotoxicity of pyridinyl and naphthalenyl analogs. *Med. Chem.* 3(2007) 115–119. doi:10.2174/157340607780059530.
- [14] D.G. Powers, D.S. Casebier, D. Fokas, W.J. Ryan, J.R. Troth, D.L. Coffen, Automated parallel synthesis of chalcone-based screening libraries, *Tetrahedron* 54 (1998) 4085–4096, doi:10.1016/S0040-4020(98)00137-9.
- [15] E. Perozo-Rondón, R.M. Martín-Aranda, B. Casal, C.J. Durán-Valle, W.N. Lau, X.F. Zhang, K.L. Yeung, Sonocatalysis in solvent free conditions: An efficient eco-friendly methodology to prepare chalcones using a new type of amino grafted zeolites, *Catalysis today* 114 (2006) 183–187, doi:10.1016/j.cattod.2006.01.003.
- [16] P.J. Tejkiran, M.S. Brahmateja, P. Sai Siva Kumar, S. Pranitha, Philip Reji, S. Naveen, N.K. Lokanath, S. Prathap Chandran, G. Nageswara Rao, D-A- π -D Synthetic approach for thienyl chalcones – NLO – a structure activity study, *J. Pho. Chem. Pho. Bio. A: Inside Chem.* 324 (2016) 33–39, doi:10.1016/j.jphtchem.2016.03.009.
- [17] S. Naveen, J. Jamal, Ming Liew Suk, C.S. Anandakumar, N.K. Lokanath, Synthesis, characterization, structural elucidation and Hirshfeld surface analysis of (E)-3-(3-methylthiophen-2-yl)-1-(pyrazin-2-yl)prop-2-en-1-one, *Chem. Data Coll* 78 (2016) 58–67, doi:10.1016/j.cdc.2017.01.004.
- [18] M.G. Prabhudeva, S. Bharath, A. Dileep Kumar, S. Naveen, N.K. Lokanath, B.N. Mylarappa, K. Ajay Kumar, Design and environmentally benign synthesis of novel thiophene appended pyrazole analogues as anti-inflammatory and radical scavenging agents: crystallographic, *in silico* modeling, docking and SAR characterization, *Bioorg. Chem.* 73 (2017) 109–120, doi:10.1016/j.bioorg.2017.06.004.
- [19] B. Pramodh, N.K. Lokanath, S. Naveen, P. Nares, S. Ganguly, J. Panda, Molecular structure, Hirshfeld surface analysis, theoretical investigations and non-linear optical properties of a novel crystalline chalcone derivative: (E)-1-(5-bromothiophen-2-yl)-3-(p-tolyl) prop-2-en-1-one, *J. Mol. Struct.* 1161 (2018) 9–17, doi:10.1016/j.molstruc.2018.01.078.
- [20] Rigaku, NUMABS, Rigaku Corporation, Tokyo, Japan, 1999.
- [21] Rigaku, Crystal Clear, 2011
- [22] Bruker (2000) SHELXTL (Version 6.10), Saint-Plus (Version 6.02) and Smart-WNT2000 (Version 5.622) Bruker AXS Inc, Madison, Wisconsin, USA. 2000
- [23] G.M. Sheldrick, Crystal structure refinement with SHELXL, *Acta Cryst.* C71 (2015) 3–8, doi:10.1107/S2053229614024218.
- [24] A.L. Spek, *Acta Crystallogr.* A46 (1990) c34 c34.
- [25] C.F. Macrae, I.J. Bruno, J.A. Chisholm, P.R. Edgington, P. McCabe, E. Pidcock, L.M. Rodriguez, R. Taylor, J. van de Streek, P.A. Wood, Mercury CSD 2.0-new features for the visualization and investigation of crystal structures, *J. Appl. Cryst.* 41 (2008) 466–470, doi:10.1107/S0021889807067908.
- [26] M.J. Frisch, G.W. Trucks, H.B. Schlegel, G.E. Scuseria, M.A. Robb, J.R. Cheeseman, G. Scalmani, V. Barone, G.A. Petersson, H. Nakatsuji, X. Li, M. Caricato, A.V. Marenich, J. Bloino, B.G. Janesko, R. Gomperts, B. Mennucci, H.P. Hratchian, J.V. Ortiz, A.F. Izmaylov, J.L. Sonnenberg, D. Williams-Young, F. Ding, F. Lipparini, F. Egidi, J. Goings, B. Peng, A. Petrone, T. Henderson, D. Ranasinghe, V.G. Zakrzewski, J. Gao, N. Rega, G. Zheng, W. Liang, M. Hada, M. Ehara, K. Toyota, R. Fukuda, J. Hasegawa, M. Ishida, T. Nakajima, Y. Honda, O. Kitao, H. Nakai, T. Vreven, K. Throssell, J.A. Montgomery, J.E. Peralta, F. Ogliaro, M.J. Bearpark, J.J. Heyd, E.N. Brothers, K.N. Kudin, V.N. Staroverov, T.A. Keith, R. Kobayashi, J. Normand, K. Raghavachari, A.P. Rendell, J.C. Burant, S.S. Iyengar, J. Tomasi, M. Cossi, J.M. Millam, M. Klene, C. Adamo, R. Cammi, J.W. Ochterski, R.L. Martin, K. Morokuma, O. Farkas, J.B. Foresman, D.J. Fox, Gaussian 16, Revision C.01, Gaussian, Inc., Wallingford CT, 2016 <https://gaussian.com/g16citation/>.
- [27] Roy Dennington, Todd A. Keith, M. John, Millam, GaussView, Version 6.1, Semichem Inc., Shawnee Mission, KS, 2016 <https://gaussian.com/Gaussview6/citation/>.
- [28] S.K. Wolff, D.J. Grimwood, J.J. McKinnon, M.J. Turner, D. Jayatilaka, M.A. Spackman, *CrystalExplorer (Version 3.1)*, University of Western Australia, 2012.
- [29] S. Sherzaman, M.N. Ahmed, B.A. Khan, T. Mahmood, K. Ayub, M.N. Tahir, Thiobiuret based Ni(II) and Co(III) complexes: synthesis, molecular structures and DFT studies, *J. Mol. Struct.* 1148 (2017) 388–396, doi:10.1016/j.molstruc.2017.07.054.
- [30] B. Evranos Aksöz, R.I. Ertan, *FabAd, chemical and structural properties of Chalcones*, *FABAD J. Pharm. Sci.* 36 (2011) 223–242.
- [31] R.G. Parr, L.V. Szentpaly, S. Liu, Electrophilicity index, *J. Am. Chem. Soc.* 121 (1999) 1922–1924, doi:10.1021/ja983494x.
- [32] R.G. Parr, R.A. Donnelly, M. Levy, W.E. Palke, *J. Chem. Phys.* 68 (1978) 3801–3807, doi:10.1021/ja004105d.
- [33] P.K. Chattaraj, U. Sarkar, D.R. Roy, Electrophilicity index, *Chem. Rev.* 106 (2006) 2065–2091, doi:10.1021/cr078014b.
- [34] A. Lesar, I. Milosev, Density functional study of the corrosion inhibition properties of 1,2,4-triazole and its amino derivatives, *Chem. Phys. Lett.* 483 (2009) 198–203, doi:10.1016/j.cplett.2009.10.082.
- [35] N.R. Sheela, S. Muthu, S. Sampathkrishnan, Molecular orbital studies (hardness, chemical potential and electrophilicity), vibrational investigation and theoretical NBO analysis of 4-(1H-1,2,4-triazol-1-yl methylene) dibenzonitrile based on abinitio and DFT methods., *Spectrochim. Acta Part A* 120 (2014) 237–251, doi:10.1016/j.saa.2013.10.007.
- [36] R. Parthasarathi, V. Subramanian, D.R. Roy, P.K. Chattaraj, Electrophilicity index as a possible descriptor of biological activity., *Bioorg. Med. Chem.* 12 (2004) 5533–5543, doi:10.1016/j.bmc.2004.08.013.
- [37] M.N. Tahir, M. Khalid, A. Islam, S.M.A. Mashhadi, A.A.C. Braga, Facile synthesis, single crystal analysis, and computational studies of sulfanilamide derivatives., *J. Mol. Struct.* 1127 (2017) 766–776, doi:10.1016/j.molstruc.2016.08.032.
- [38] P. Politzer, Atomic and molecular energies as functionals of the electrostatic potential, *Theor. Chem. Acc.* 111 (2004) 395–399, doi:10.1007/s00214-003-0533-4.
- [39] D.A. Zainuri, I.A. Razak, S. Arshad, Molecular structure, DFT studies and Hirshfeld analysis of anthracenyl chalcone derivatives, *Acta Cryst. E*: 74 (2008) 780–785, doi:10.1107/S2056989018006527.
- [40] K. Arulaabaranam, S. Muthu, G. Mani, S. Sevvanthi, Quantum mechanical computation, spectroscopic exploration and molecular docking analysis of 2-Bromo-4-fluoroacetanilide, *J. Mol. Struct.* (2020) 128639, doi:10.1016/j.molstruc.2020.128639.